Temperature dependence of the spin relaxation time of donor-bound electrons immersed in a CdTe quantum well

G. Garcia-Arellano,[1] F. Bernardot,[1] G. Karczewski,[2] C. Testelin,[1] and M. Chamarro[1]
[1]*Sorbonne Université, CNRS, Institut des NanoSciences de Paris, 4 place Jussieu, F-75005 Paris, France*
[2]*Institute of Physics, Polish Academy of Sciences, Al. Lotników 32/46, PL-02668 Warsaw, Poland*

(Received 30 July 2019; revised manuscript received 20 September 2019; published 25 November 2019)

The behavior of the spin relaxation time of electrons bound to donors immersed in the middle of a CdTe quantum well was measured in the range of temperatures 10–80 K, by using picosecond pump-probe Kerr rotation. Different doping concentrations spanning from isolated donors up to a concentration beyond the metal-insulator transition were considered at a fixed magnetic field; at very low temperature, in insulating regime all electrons are bound to donors but for one high concentration we had to consider that a fraction of electrons is in conduction states. By increasing the temperature, the number of conduction electrons increases. The experimental temperature dependences were explained by invoking spin exchange between electron spins localized on donors and the spin of electrons promoted to conduction states. A good agreement between experiment and theory was found and allowed us to conclude that, while the spin of localized electrons undergoes the effect of both hyperfine and anisotropic exchange interactions, the D'yakonov-Perel' mechanism governs the spin relaxation of the conduction electrons for the whole range of the studied doping concentrations. Moreover, we identified the scattering mechanisms possibly undergone by the conduction electrons at low temperature.

DOI: 10.1103/PhysRevB.100.205305

I. INTRODUCTION

Spin dynamics and the related physics have been the center of a renewed attention since the possibility to obtain novel spin electronic devices has been open [1,2]. One of the major challenges currently faced is obtaining long spin lifetimes. Among the many systems that have been studied for applications in classical and quantum technologies, semiconductors are very suitable because their electronic doping leads to long spin relaxation times. Consequently, a huge effort to understand the different mechanisms involved in the electronic spin relaxation has been made [3–8].

Presently, a clear picture of spin relaxation mechanisms in n-doped bulk zinc-blende materials exists at low temperatures and doping concentrations well above the metal-insulator transition (MIT), for any concentration at high temperatures, where all the electrons are delocalized, and at low temperatures in the insulating regime. In the first two situations, at least for materials with small spin-orbit interaction, as the most studied one GaAs, the D'yakonov-Perel' (DP) mechanism is the dominant one. The lack of inversion symmetry and the spin-orbit interaction lead to an effective $\vec{k}$-dependent magnetic field; as a consequence the spin of electrons in conduction states precesses about an axis related to $\vec{k}$, which leads to spin relaxation. The precession axis changes at each scattering process, and then the spin relaxation rate due to this mechanism is inversely proportional to the rate of scattering [9].

At low temperatures and in the insulating regime, i.e., for localized electrons, the spin relaxation time has been explained as an interplay of different mechanisms whose probability depends on doping concentration [7,8,10,11]. At low doping concentration, when donors can be considered isolated from each other, the hyperfine interaction with nuclear spins dominates the electron spin relaxation [5]. Then, as the concentration is increased, an interplay between the hyperfine interaction and the anisotropic exchange governs the electron-spin relaxation. This latter interaction is a part of the exchange interaction that induces spin rotation in opposite directions of two adjacent localized electron spins, when these two electrons tunnel from one of the donors to the other in an effective spin-orbital field. For higher doping levels below the MIT, the anisotropic exchange interaction becomes the principal mechanism. The understanding is less established for concentrations in the metallic region near the MIT transition at low temperatures because the situation is more complex [12–14] due to the coexistence of localized electrons in a band of impurities and itinerant electrons leading to filamentary electron transport [15,16]. Recently, several calculations have attempted to describe spin relaxation beyond the MIT [17,18] based on the model of Matsubara and Toyozawa [19]. The description of spin relaxation at low temperatures near the MIT implies a fundamental understanding of the spatial dynamics of the electrons [15]. Wellens and Jalabert have described lately the hopping dynamics of electrons in a disordered network of impurity sites [20], but more theoretical work is needed in this direction.

In order to describe the spin relaxation behavior as a function of temperature in *n*-doped zinc-blende materials, Putikka and Joynt [21] have considered a cross relaxation between localized and itinerant spins by exchange interaction. The interaction between electrons in the impurity band and electrons in the conduction band was proposed in a very early work of Paget for highly pure GaAs under light excitation [22]. Indeed, by increasing temperature the number of ionized

donors increases and two kinds of electrons can be considered: localized and itinerant electrons. Recently, such an approach has been extended to wurtzite materials as ZnO [23] and low-dimensional systems; in particular, Harmon *et al.* have described the unusual temperature dependence of spin relaxation time in (110)-GaAs quantum wells (QWs) [24].

In this work, we perform a study of the temperature behavior of the spin relaxation time undergone by donor-bound electrons, for temperatures between 10 and 80 K and in a doping range spanning from 3.2×10^{10} to 3.6×10^{11} donors cm^{-2} and at a fixed magnetic field. Iodine donors are immersed in the center of an 8-nm CdTe/CdMgTe QW. This system emerged some years ago as a good prototype for spintronic applications, since experimental studies revealed that the localization of the electron wave function leads to an enhancement of the spin relaxation time. Besides, they present a higher degree of optical orientation of the electron spins than in three-dimensional crystals, and the integration of impurities does not lead to large inhomogeneities [25–28]. We have adapted the formalism used in Ref. [24] to describe the temperature dependence of the spin relaxation in the insulating regime and for one sample with a doping concentration slightly beyond the Mott transition. We used the expression of the spin relaxation rate due to the DP mechanism valid for any temperature by Kainz *et al.* [29]. We found a good agreement between theory and experiment. We deduced that the DP mechanism governs the spin relaxation time of the conduction electrons for all samples, and that the dominant scattering type, according to the classification made by Ref. [29] of the different scattering mechanisms, is the type I for all studied concentrations.

II. SAMPLES AND EXPERIMENTAL SETUP

The four samples studied here consist of a CdTe/CdMgTe heterostructure grown by molecular-beam epitaxy on a (100)-oriented GaAs substrate containing an 80-Å CdTe QW. The samples were doped with iodine atoms placed in the midplane of the QW, each with a different doping concentration: (A) $3.2\times10^{10}\,\mathrm{cm}^{-2}$, (B) $9.7\times10^{10}\,\mathrm{cm}^{-2}$, (C) $2.9\times10^{11}\,\mathrm{cm}^{-2}$, and (D) $3.6\times10^{11}\,\mathrm{cm}^{-2}$. To study the spin dynamics of resident electrons, we use a pump-probe technique, the photoinduced Kerr rotation, in which an optical heterodyne amplification of a probe beam is detected [30]. The light source is a Ti:sapphire laser beam with pulses of 2-ps duration and a repetition rate of 76 MHz, which is split into pump, probe, and reference beams. Pump and probe beams are focused on the sample with a microscope objective (numerical aperture = 0.5) giving a spot diameter of 1 μm. The pump beam is $\sigma+/\sigma-$ modulated at 42 kHz with a photoelastic modulator, in order to avoid nuclear spin polarization via electronic spins optically oriented by the pump. Probe and reference beams are linearly polarized and passed across two different acousto-optic modulators. Then, the first diffraction orders of both beams undergo an optical frequency shift $f_1 = 110$ MHz (probe) and $f_2 = 112$ MHz (reference). After interaction with the sample, the reflected probe beam is superposed to the reference beam in an avalanche photodiode, and the heterodyne signal modulated at 2 MHz is detected by using a double-stage lock-in amplifier. The signal corresponding to the spin polarization of the donor-bound electrons is hence obtained with a high pump/signal rejection. The sample is mounted in a cryostat with a closed circuit of liquid helium, that allows to vary its temperature between 5 and 120 K. We used permanent magnets to apply a fixed magnetic field perpendicular to the pump and probe beams (Voigt configuration).

III. PHOTOLUMINESCENCE SPECTRA AND SPIN DYNAMICS OF DONOR-BOUND ELECTRONS AS A FUNCTION OF THE TEMPERATURE

Figure 1(a) shows the photoluminescence (PL) spectra recorded for sample B at different temperatures. At low temperatures, the PL is dominated by a band centered at 1.611 eV and associated with the recombination of the donor-bound exciton (D^0X). A second peak at higher energy, 1.616 eV, is also observed and is identified as the free-exciton (X) contribution. As the temperature is increased, both features are shifted to lower energies and the widths of the bands increase. Figure 1(b) shows the evolution of the energy peaks appearing in the PL of sample B, as a function of the temperature. It is essentially fixed by the evolution of the CdTe QW energy band gap. We observe that the D^0X band merges with the X one above 60 K. We partly explain this phenomenon by the thermal activation of the D^0X population. We write the variation of the D^0X population with the temperature according to the equation

$$n(T) = \frac{n_0}{1+\exp\left(-\frac{E_l}{k_B T}\right)}, \tag{1}$$

where $n(T)$ represents the D^0X population at temperature T, n_0 represents the D^0X population at $T = 0\,\mathrm{K}$, and E_l is the binding energy of X on D^0 in the D^0X complex. The binding energy E_l is given by the difference between the D^0X and X lines observed in the PL. Taking the average value of this energy difference, we find $E_l = 3.7\,\mathrm{meV}$; so at $T = 60\,\mathrm{K}$ we have $n = 0.7\,n_0$, meaning that 30% of the bound excitons have joined the population of free excitons. Figure 1(c) shows the PL spectra for sample D, which has a doping concentration slightly above the Mott transition, according to the Mott criterion [38] and previous studies [10]. We underline that these PL spectra are broad; contrary to the sample B, we cannot distinguish separate emissions from donor-bound and free excitons.

The photoinduced Kerr rotation signal obtained on sample B at the temperature $T = 50\,\mathrm{K}$, under a magnetic field $B = 0.56\,\mathrm{T}$, is shown in Figs. 2(a) and 2(b) when the pump-probe energy is, respectively, at the D^0X and X transitions. In both cases, an oscillatory and long-lasting signal is observed. This oscillatory signal, with an envelope time larger than the lifetime of the D^0X complex ($T_R \sim 200\,\mathrm{ps}$ [27]), is the signature of the spin polarization of electrons bound to donors, D^0 [26]. We underline that a longer long-lasting signal is observed when the excitation is done at the D^0X transition. This is in agreement with theoretical arguments in the sense of a nonresonant excitation (at higher energies) creating other species that shorten the spin relaxation time [7].

We have studied the temperature evolution of the spin dynamics in samples A, B, C, and D. Tuning pump and probe energies at the D^0X transition, we create mainly

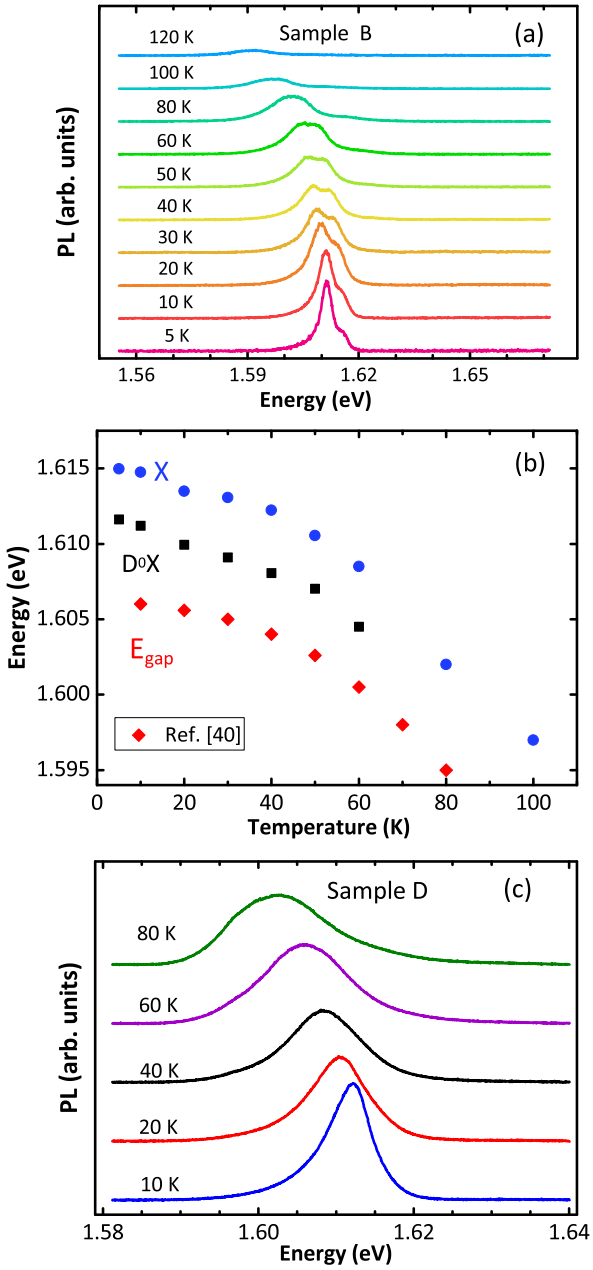

FIG. 1. (a) PL spectra of sample B, for temperatures ranging from 5 to 120 K. (b) Variations with temperature of the peak energies in the PL spectra, for sample B; X: exciton line; D^0X: donor-bound exciton line; $E_{\rm gap}$: gap energy. (c) PL spectra of sample D, for temperatures ranging from 10 to 80 K.

donor-bound excitons, since the bandwidth of the used mode-locked Ti:sapphire laser is less than 1 meV. Figures 3(a)–3(d) represent the photoinduced Kerr rotation signal obtained in samples A–D, respectively, in the 10–80 K range. Two components are visible in each curve. To extract the times and relative amplitudes of the short- and long-living components, we have fitted each curve with a biexponential function:

$$y(t) = A_1 e^{-(t/\tau_1)} \cos(\omega_1 t) + A_2 e^{-(t/\tau_2)} \cos(\omega_2 t), \qquad (2)$$

where A_1 and A_2 are constants describing the amplitudes of the fast (τ_1) and slow (τ_2) components with Larmor frequencies

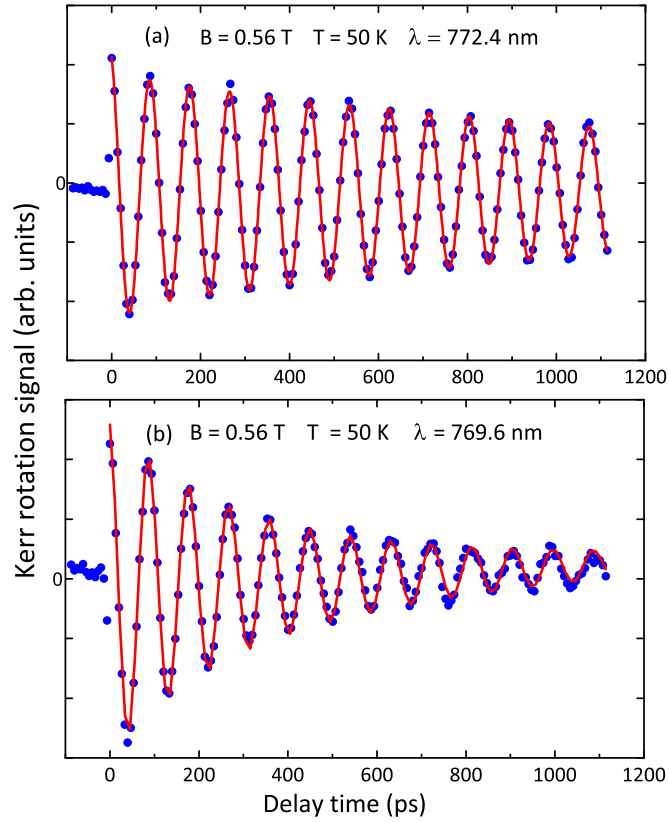

FIG. 2. Photoinduced Kerr rotation signals for sample B, in a magnetic field $B = 0.56$ T, at 50 K. Pump and probe energies are tuned to the wavelength (a) $\lambda = 772.4$ nm, D^0X transition; (b) $\lambda = 769.6$ nm, X transition. Blue full disks: experimental data; red continuous lines: fits with Eq. (2).

ω_1 and ω_2, respectively. The fast component is associated with the exciton contribution, and the second one with the D^0 contribution. The component related with the exciton contribution becomes more evident at high temperature.

In all the samples, the spin dephasing time τ_2 of electrons bound to donors becomes shorter as the temperature is increased. Sample B shows slower decays at all temperatures. In particular, at low temperatures 10–30 K, it exhibits almost no decay in the 1-ns measurement window, making the determination of the spin dephasing time less accurate.

IV. SPIN RELAXATION TIME

A. Localized electrons

At low temperature, the mechanisms that are at the origin of the spin relaxation of localized electrons at a given concentration are well known in bulk and QW systems [8,10]. The dependence on temperature of these mechanisms has been shown to be very weak [21].

In the insulating regime, at residual doping concentrations, the localized spins relax due to hyperfine interaction with nuclear spins. A localized electron is coupled to many nuclear spins by the hyperfine interaction. These nuclear spins act as a local magnetic field whose orientation and intensity depend on the considered donor site. The spin relaxation time for samples in this regime is given by the dephasing time T_Δ^e [5].

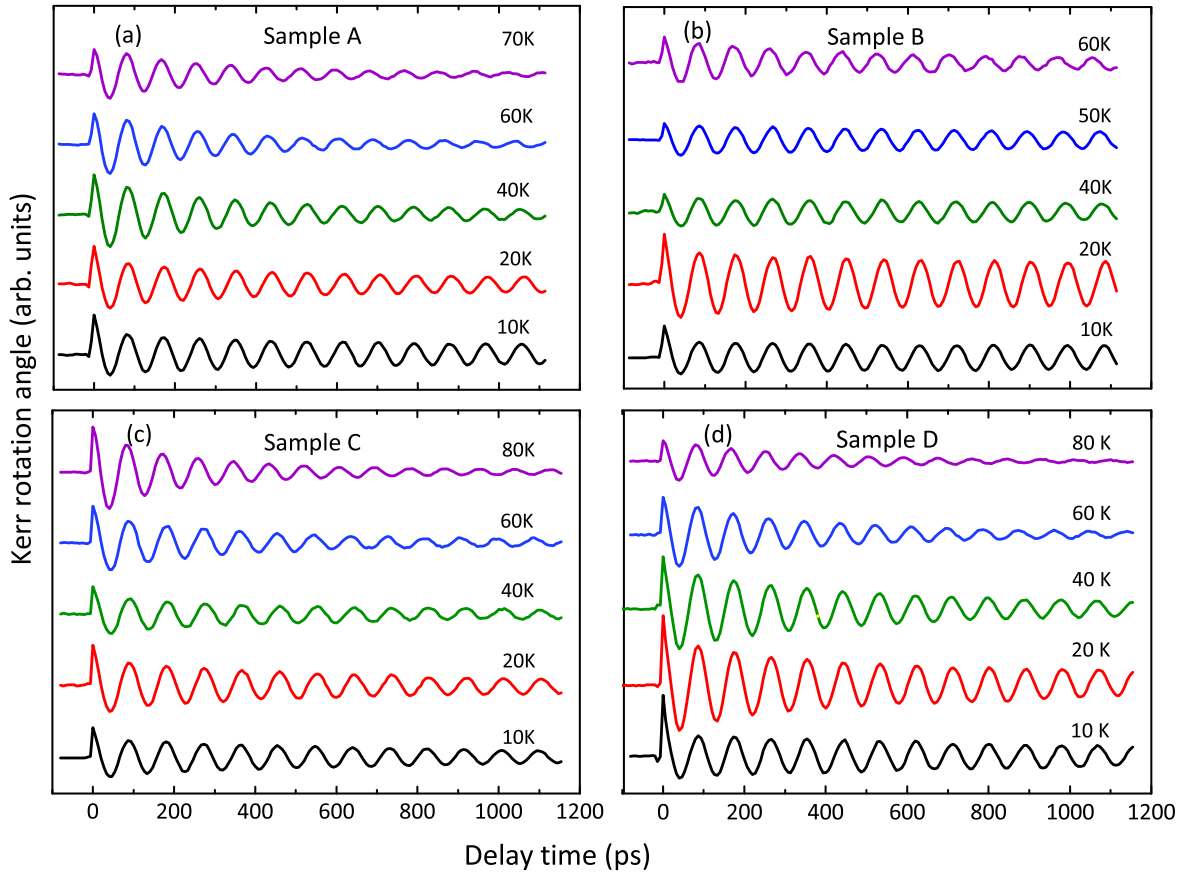

FIG. 3. Photoinduced Kerr rotation signals in a magnetic field $B = 0.56$ T, at different temperatures, in (a) sample A; (b) sample B; (c) sample C; and (d) sample D. Pump and probe energies are tuned to the D^0X transitions.

For a CdTe QW of thickness equal to $L = 8$ nm, T^e_Δ has been estimated to be 5.6 ns [10].

As the doping concentration increases, the electron wave functions begin to overlap; the spin of an electron is no longer localized on a single donor and interacts with other donors. As a result, the effect of nuclear-spin fluctuations become smaller and the relaxation time increases [8,10]. The expression for the spin relaxation time τ_{sn} in this regime is proportional to the square of T^e_Δ, and is inversely proportional to the residence time of the electron spin on a given donor site, $\tau_{\rm corr}$, which is a function of the exchange constant $J(r)$ [8].

For high doping concentrations, a strong overlap of the electron wave functions is accompanied with an increase of probability that the electron spin relaxes due to the anisotropic exchange interaction. During each exchange, there is a rotation of an angle θ, simultaneous and in the opposite direction, for each of the two electron spins that exchange their positions on the donors. Eventually, for the highest doping concentration in the insulating regime, the anisotropic exchange interaction becomes stronger than the hyperfine interaction, and the rise of the spin lifetime with concentration is changed for a decrease. The expression for the spin relaxation time τ_{sa} due to this mechanism is proportional to $\tau_{\rm corr}$ and inversely proportional to the square of θ [8]. The corresponding expressions for θ in semiconductor QWs and bulk is given in Refs. [31,32].

Taking into account the hyperfine and anisotropic exchange interaction, the spin relaxation time for any doping concentration in the insulating regime at low temperature is given by

$$\tau_l = \left(\frac{1}{\tau_{sn} + T^e_\Delta} + \frac{1}{\tau_{sa}}\right)^{-1}. \tag{3}$$

B. Conduction electrons

The DP theory has been recently generalized to describe the spin relaxation time for an electron gas in a QW at any temperature [29]. The spin relaxation time is written as a function of the temperature via the Fermi distribution function and the temperature dependence of the transport mobility:

$$\frac{1}{\tau_c} = \frac{4}{\hbar^2}\frac{\beta E_F \tau_{\rm tr}}{1 - e^{-\beta E_F}}\left[\gamma^2\langle k_z^2\rangle^2\frac{\zeta}{\beta} - \frac{\gamma^2\langle k_z^2\rangle}{2}\left(\frac{\zeta}{\beta}\right)^2\frac{J_{\nu+2}(\beta\mu_0)}{J_{\nu+1}(\beta\mu_0)}\right.$$
$$\left. + \left(1 + \frac{\tau_3}{\tau_1}\right)\gamma^2\left(\frac{\zeta}{\beta}\right)^3\frac{J_{\nu+2}(\beta\mu_0)}{J_{\nu+1}(\beta\mu_0)}\right], \tag{4}$$

where $\mu_0 = k_B T\ \ln(e^{E_F/k_B T} - 1)$ is the chemical potential, $E_F = \frac{\hbar^2\pi}{m^*}n_c$ is the Fermi energy, with m^* the effective electron mass and n_c the concentration of conduction electrons in 2D, γ is the Dresselhaus coefficient which can be calculated from the spin-orbit constant [10], $\langle k_z^2\rangle$ is the average value

of the squared z component of the electron wave vector, $\zeta = 2m^*/\hbar^2$, $\beta = 1/k_BT$, τ_3/τ_1 is a constant describing the angular scattering characteristics of the scattering mechanism, and $\tau_{\rm tr}$ is the transport collision time given by

$$\tau_{\rm tr} = \frac{\Xi J_{\nu+1}(\beta\mu_0)}{\beta^{\nu+1}E_F}, \tag{5}$$

with $J_n(z) = \int_0^\infty \frac{x^n}{4\cosh^2(\frac{x-z}{2})}dx$ and Ξ a coefficient that varies slightly with the temperature, independent of energy, and related with the power-law dependence of τ_1 on the energy. The index ν takes the values 0, 1, or 2 depending on the scattering type [29]. Each type of scattering encloses different scattering mechanisms, e.g., type I is associated with acoustic phonons, optical phonons, screened ionized impurities, neutral impurities, alloy scattering, and interface roughness [29].

C. Temperature behavior of spin relaxation of localized electrons

The temperature dependence of the spin relaxation time for an electron localized on donor has been explained in bulk and QWs invoking spin exchange between two spin species: spin localized on donors, and spin carried by itinerant electrons [21–24].

At low temperatures, the donors are nearly all occupied and the electron spins are localized. As the temperature is increased, the number of conduction electrons increases due to the thermal ionization of the electron bound to donors. The electronic spins localized on the donors interact with the spin of conduction electrons by isotropic exchange interaction. This interaction conserves the total spin; assuming that the cross relaxation is fast enough, the total spin is equilibrated between localized and conduction electrons by taking into account their thermal equilibrium concentrations. Taking into account the existence of these two spin systems, the spin relaxation rate of donor-bound electrons at zero magnetic field is found in the form [24]

$$\frac{1}{\tau_s} = \frac{n_l}{n_{\rm imp}}\frac{1}{\tau_l} + \frac{n_c}{n_{\rm imp}}\frac{1}{\tau_c}, \tag{6}$$

where $n_l(T)[n_c(T)]$ is the localized [conduction] equilibrium concentration, $n_{\rm imp} = n_l + n_c$ is the total impurity concentration, and τ_l (τ_c) is the localized (conduction) spin relaxation time. $n_l(T)$ can be determined exactly in two dimensions (2D), at any temperature [33]:

$$\frac{n_l(T)}{n_{\rm imp}} = \frac{\sqrt{1+Q(T,n_{\rm imp})} - 1}{\sqrt{1+Q(T,\ n_{\rm imp})} + 1}, \tag{7}$$

with $Q(T, n_{\rm imp}) = \frac{8n_{\rm imp}}{N_c}e^{-(E_b/k_BT)}$, $N_c = m^*k_BT/\hbar^2\pi$, and E_b the binding energy of an electron bound to a donor. $n_c(T)/n_{\rm imp}$ can be found using the constraint:

$$\frac{n_l(T)}{n_{\rm imp}} + \frac{n_c(T)}{n_{\rm imp}} = 1. \tag{8}$$

For vanishing temperatures, when $n_{\rm imp}$ is on the range of the insulating regime, $n_l(T)$ goes to $n_{\rm imp}$ and $n_c(T)$ goes to zero. However, as we will explain later, $n_c(0) \neq 0$ when $n_{\rm imp}$ is above the MIT. The spin relaxation mechanisms for localized and conduction electrons that govern the times τ_l and τ_c appearing in Eq. (6) are in principle the same as at low temperature. For localized electrons, τ_l is determined by Eq. (3), while for conduction electrons, the DP mechanism governs the spin relaxation time [Eq. (4)].

V. DISCUSSION OF THE RESULTS

We have experimentally determined in our four samples, for the temperature range 10–80 K, the long-lasting spin dephasing time τ_2 [see Eq. (2)] at a fixed magnetic field of $B = 0.56$ T. The experimentally measured dephasing time is affected by inhomogeneities caused by the local variations of the electron g_e factors. τ_2 is related with the spin relaxation time τ_s of a single electron by the expression

$$\frac{1}{\tau_2} = \frac{1}{\tau_s} + \frac{\Delta g_e \mu_B B}{\hbar}. \tag{9}$$

The width Δg_e of the g_e distribution for each sample has been determined in a previous work [10]. We have fitted the measured τ_2^{-1} for samples A to D with Eq. (9) using τ_s^{-1} given by the model proposed by Harmon *et al.* [24] [Eq. (6)]. We have neglected the inhomogeneities of g_e factors for conduction electrons, because in a previous work on an 8-nm CdTe QW containing a 2D electron gas [34], the spin relaxation time of conduction electrons was shown to be negligibly sensitive to these inhomogeneities.

A. Insulating regime

For samples A, B, and C in the insulating regime, the spin dephasing rate τ_2^{-1} is shown in Figs. 4(a)–4(c). We consider that the conduction electrons relax according to the DP mechanism [Eq. (4)]. In order to identify which type of scattering is dominant, we have fitted the experimental data scanning the values $\nu = 0$, 1, and 2 in Eq. (4). In this regime, the Fermi energy varies with the temperature-dependent concentration $n_c(T)$, determined by Eqs. (7) and (8). For each sample, the parameters to be determined are the binding energy E_b, the spin dephasing time τ_l^* ($1/\tau_l^* = 1/\tau_l + \Delta g_e\mu_B B/\hbar$) of the ensemble of localized electrons, and the coefficient Ξ (assumed to be a constant independent of T).

In Fig. 4, the blue solid line shows the spin dephasing rate τ_2^{-1} as a function of the temperature, according to Eqs. (6) and (9), and using the type-I scattering ($\upsilon = 0$). Since it is impossible to fit the experimental data assuming type-II ($\upsilon = 1$) or type-III ($\upsilon = 2$) scatterings, we can firmly identify the type-I scattering as the effective one in the studied samples. Table I gives the fitting parameters E_b, τ_l^*, and Ξ for all studied samples.

At low temperatures, it has been shown that the mechanism that governs the spin relaxation in sample A (with a low-doping concentration) is the hyperfine interaction [10]. In Ref. [10], the binding energy for an isolated donor has been calculated to be $E_b = 24.7$ meV in sample A. Taking this theoretical value as a starting point, we have fitted the experimental data for sample A, with only τ_l^* and Ξ as free parameters [see the dashed line in Fig. 4(a)]. We have obtained $\tau_l^* = 1.47 \pm 0.05$ ns and $\Xi = 146$ fs. As shown in Fig. 4(a), a lower binding energy is needed to agree better with the experimental results; the solid line represents the spin dephasing

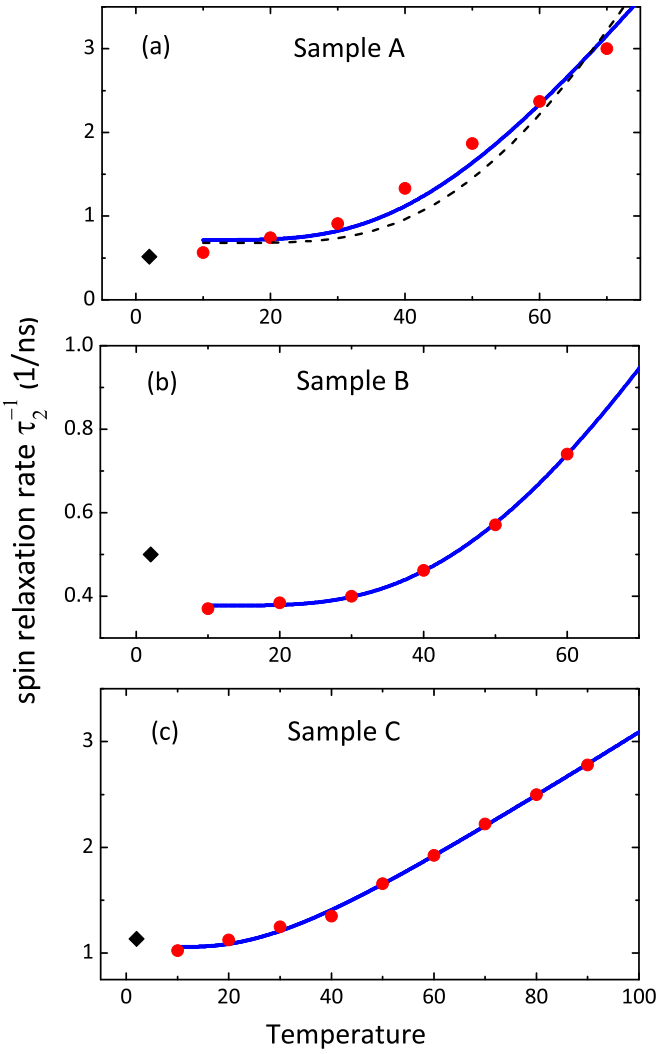

FIG. 4. Measurements of the spin dephasing rates at different temperatures (red full disks) in (a) sample A; (b) sample B; and (c) sample C. The blue continuous lines are theoretical fits according to Eqs. (6), (7), and (9), for the type-I scattering ($\nu = 0$). The fitting parameters are given in Table I. The dashed line in (a) is a theoretical fit forcing $E_b = 24.7$ meV. The black full diamonds are data points extracted from Ref. [10].

time considering a lower binding energy, $E_b = 19$ meV. The value extracted for the spin dephasing time of the localized electrons, $\tau_l^* = 1.40$ ns, compares well with 1.97 ns obtained in a previous work [10] in the same magnetic field $B = 0.56$ T, at 2 K [black diamond in Fig. 4(a)].

In Eq. (7), the concentrations $n_l(T)$ and $n_c(T)$ of localized and conduction electrons have a strong dependence on the binding energy. The smaller the binding energy, the lower the electron ionization temperature. In QWs, there is no theory that predicts a value for the binding energy at any doping concentration. Nonetheless, in bulk systems it has been generally shown, theoretically and experimentally, that the binding energy decreases when the doping concentration increases [13,35–37].

As can be seen in Fig. 5(a), right axis, the density of conduction electrons in sample A starts to increase at a

TABLE I. Extracted parameters from the fits of the experimental data for the spin relaxation time as function of the temperature; see Figs. 4 and 6(a). For sample D, the values are obtained considering a concentration of conduction electrons $n_c(0) = 0.1\ n_{\rm imp}$ at zero temperature.

Sample	Doping concentration $n_{\rm imp}$ (cm^{-2})	Spin dephasing time τ_l^* (ns)	Binding energy E_b (meV)	Transport coefficient Ξ (fs)
A	3.2×10^{10}	1.40 ± 0.05	19 ± 1	97
B	9.7×10^{10}	2.65 ± 0.05	20 ± 1	36
C	2.9×10^{11}	0.95 ± 0.05	8 ± 1	47
D	3.6×10^{11}	1.63 ± 0.05	6 ± 1	47

temperature around 25 K, and at $T = 100$ K, almost one half of the donors has been ionized. In Fig. 5(a), the conduction spin relaxation time is also plotted as a function of the temperature, with $E_b = 19$ meV and $\Xi = 97$ fs, known from the theoretical fit of Fig. 4(a). As the density of conduction

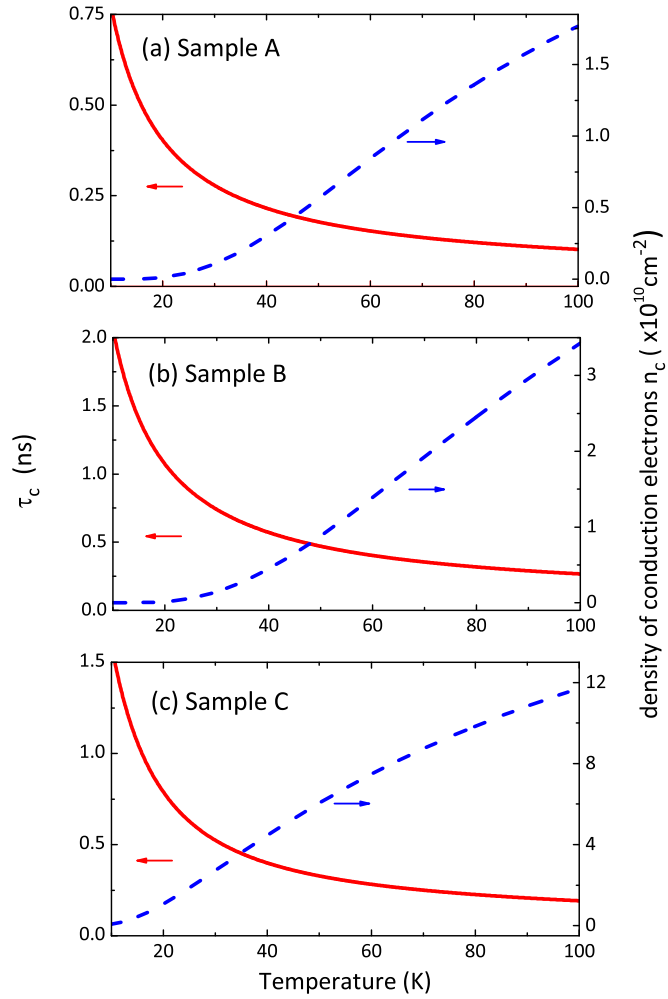

FIG. 5. Concentrations of conduction electrons (dashed lines, right axis), and spin relaxation times of the conduction electrons (continuous lines, left axis) versus temperature, in (a) sample A; (b) sample B; and (c) sample C.

electrons increases with the temperature, the spin relaxation time decreases.

Sample B contains an intermediate doping concentration, and the mechanism that governs the spin relaxation time of the localized electrons is an interplay between the hyperfine and the anisotropic exchange interaction [10]. Since there is no theory that predicts a value of the binding energy for this doping concentration, we took it as a free parameter to fit the data of Fig. 4(b). The values extracted from the theoretical fit are $E_b = 20$ meV, $\tau_l^* = 2.65$ ns, and $\Xi = 36$ fs. The value of the localized spin dephasing time τ_l^* is of the same order as the one measured in a previous work [10] (around 2 ns) at 2 K in the same magnetic field [black diamond in Fig. 4(b)]. The difference between the obtained value and the value measured in Ref. [10] may come from slightly different experimental conditions, in particular, the density of excitation.

Finally, sample C contains a doping concentration that is close to the metal-insulator transition while keeping in the insulating regime. The principal spin relaxation mechanism for localized electrons in this region is the anisotropic exchange interaction [10]. The values extracted from the theoretical fit in Fig. 4(c) are $E_b = 8$ meV, $\tau_l^* = 0.95 \pm 0.05$ ns, $\Xi = 47$ fs. The value for the localized spin dephasing time agrees well with the experimental value of 0.9 ns found at 2 K in the same magnetic field measured in a previous work [10].

For this sample C, due to the small binding energy $E_b = 8$ meV, the localized electrons start to ionize at low temperature, see Fig. 5(c). At high temperature, $T \sim 100$ K, the conduction spin relaxation time is of the order of 100 ps, see Fig. 5(c). This value compares well to the one observed in 2D electron gas of n-doped CdTe QW with a similar concentration, at low temperature [34].

We suspect that, due to the kind of the studied system (donors inside a QW) and the range of temperatures 10–80 K, scatterings with neutral impurities and with screened ionized impurities (at the highest temperature) are the more probable scattering mechanisms. But we cannot exclude other mechanisms, as for example the one related to the interface roughness. Because we worked at relatively low temperature, we exclude however the scattering due to acoustic phonons.

We underline that Fig. 5, right axis, shows the calculated density of conduction electrons as a function of the temperature, which is equal to the density of ionized impurities. Then for samples A, B, and C at the middle of the explored temperature domain, the density of ionized impurities becomes only 10 or 20% of the total amount of donors in the sample. At 80 K, the density of ionized impurities becomes larger and, in particular for sample C, can reach a value of 35% of the total amount of donors in the sample. This shows that, in the explored domain of temperatures, the donors are mostly in their neutral state. Moreover, the ionized donors are likely to be screened by conduction electrons which are confined inside the QW.

B. Metallic regime, near the MIT

Under the Mott criterion [38], and following previous studies [10], sample D is assumed to possess a doping concentration slightly beyond the MIT; conductance measurements could confirm this point, but our samples are not patterned for transport experiments. We found that the experimental data on this sample could *not* be fitted by considering only a population of conduction electrons and a dephasing time related to DP or/and Elliott-Yafet (EY) mechanisms. For doping concentrations slightly above the MIT, it has been shown that there is a coexistence between localized electrons forming an impurity band, and itinerant electrons, leading to a filamentary electronic transport [16].

In order to explain the spin dephasing time observed in sample D, we have considered that at very low temperature a fraction f of the doping concentration $n_{\rm imp}$ is in the conduction band:

$n_c(0) = f n_{\rm imp}$. Thus, at any temperature the density of localized electrons is given by a refined version of Eq. (7):

$$n_l(T) = n_l(0)\frac{\sqrt{1+Q[T,n_l(0)]}\ -\ 1}{\sqrt{1+Q[T,n_l(0)]}\ +\ 1}, \tag{10}$$

with $n_l(0) = n_{\rm imp}(1-f)$. The density of conduction electrons at any temperature is evaluated from the conservation rule $n_c(T) = n_{\rm imp} - n_l(T)$. Figure 6(a) shows the theoretical fit of the measured spin dephasing time according to Eqs. (6),

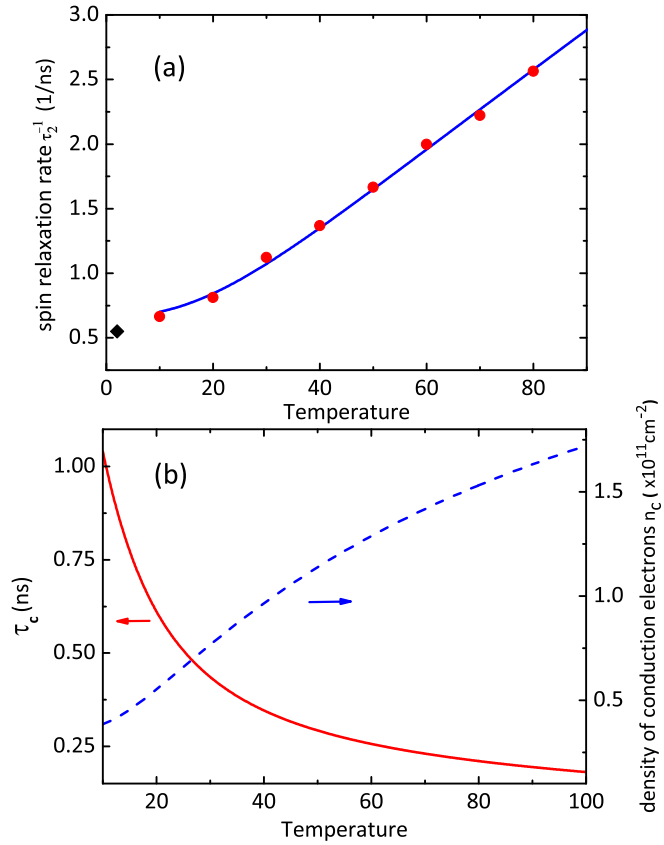

FIG. 6. (a) Measurements of the spin dephasing rates at different temperatures (red full disks) in sample D. The blue continuous line is a theoretical fit according to Eqs (6), (9), and (10), for the type-I scattering ($\nu = 0$). The fitting parameters are given in Table I. The black full diamond is a data point extracted from Ref. [10]. (b) Concentration of conduction electrons (dashed line, right axis), and spin relaxation time of the conduction electrons (continuous line, left axis) versus temperature, in sample D.

(9), and (10), and Eq. (4) for the spin relaxation time of the conduction electrons. We have taken as free parameters the binding energy E_b, the transport coefficient Ξ, the spin dephasing time τ_l^* of the localized electrons, and the fraction $f = n_c(0)/n_{\text{imp}}$ of conduction electrons at vanishing temperatures.

Scanning the values $\nu = 0,\ 1$, and 2 in Eq. (4), we identify that the type of scattering undergone by the conduction electrons in sample D is associated with collisions with neutral or screened impurities (type-I scattering, $\nu = 0$). The fitting parameters are found to be $f = 0.1$, $E_b = 6$ meV, $\tau_l^* = 1.63$ ns, and $\Xi = 47$ fs. The black diamond in Fig. 6(a) represents the spin dephasing time measured in Ref. [10] at 2 K, in the same magnetic field of $B = 0.56$ T; this value agrees well with our experimental data.

In Fig. 6(b), the conduction spin relaxation time (left axis) is plotted as a function of the temperature, with $E_b = 6$ meV and $\Xi = 47$ fs; the density of conduction electrons is also plotted (right axis). As the temperature increases, due to the small binding energy, the density of conduction electrons increases at a faster rate in comparison with the samples in the insulating regime.

For materials with a large spin-orbit constant or narrow energy band gap, the EY mechanism of spin relaxation becomes dominant for conduction electrons [24]. The spin-orbit constant of CdTe is three times larger than the one of GaAs, material for which it has been shown that EY mechanism is not effective as compared to the DP one [24]. Using $\tau_{\text{tr}} = \Xi = 47$ fs obtained here and expression (15) of Ref. [39], the DP mechanism is found more than 10 times larger than the EY one in the range of temperatures studied and for all the samples. This justifies, *a posteriori*, our use of the DP mechanism to describe the spin relaxation of conduction electrons in our samples.

VI. CONCLUSION

In summary, we have achieved a quantitative agreement between theory and experiment for the temperature dependence of the spin relaxation time of donor-bound electrons immersed in the center of an 8-nm CdTe QW, in the range of temperatures 10–80 K, by considering that two types of spin systems coexist and interact by spin exchange: the electrons localized on donors, and the free electrons promoted to the conduction band.

We evidenced that the spin relaxation time for the localized electrons is imposed by the same mechanisms known at low temperature (hyperfine and anisotropic exchange interactions), while the spin relaxation time of the conduction electrons is governed by the DP mechanism. For the samples in the insulating regime, we have identified that the scatterings undergone by the conduction electrons are of type I [29]. Under the same framework, we have succeeded in explaining the observed behavior versus temperature of the spin relaxation time for the sample with a doping concentration slightly above the Mott transition, by considering that an initial concentration of delocalized electrons exists at low temperature; the scatterings of the conduction electrons in this sample are also of type I.

ACKNOWLEDGMENTS

We acknowledge B. Eble, P. Grinberg, and B. Siarry for the development of the optical heterodyne experiment used in this study.

[1] D. D. Awschalom and M. E. Flatté, Nat. Phys. **3**, 153 (2007).
[2] F. Pulizzi, Nature Physics **4**, S20 (2008).
[3] G. E. Pikus and A. N. Titkov, in *Optical Orientation*, edited by F. Meier and B. P. Zakharchenya (North-Holland, Amsterdam, 1984).
[4] M. I. D'yakonov, *Spin Physics in Semiconductors* (Springer-Verlag, Berlin, 2008).
[5] I. A. Merkulov, Al. L. Efros, and M. Rosen, Phys. Rev. B **65**, 205309 (2002).
[6] K. V. Kavokin, Phys. Rev. B **64**, 075305 (2001).
[7] K. V Kavokin, Semicond. Sol. Technol. **23**, 114009 (2008).
[8] R. I. Dzhioev, K. V. Kavokin, V. L. Korenev, M. V. Lazarev, B. Ya. Meltser, M. N. Stepanova, B. P. Zakharchenya, D. Gammon, and D. S. Katzer, Phys. Rev. B **66**, 245204 (2002).
[9] M. I. D'yakonov and V. I. Perel', Zh. Eksp. Teor. Fiz. **65**, 362 (1973) [Sov. Phys. JETP **38**, 177 (1974)].
[10] G. Garcia-Arellano, F. Bernardot, G. Karczewski, C. Testelin, and M. Chamarro, Phys. Rev. B **99**, 235301 (2019).
[11] G. Garcia-Arellano, F. Bernardot, C. Testelin, and M. Chamarro, Phys. Rev. B **98**, 195308 (2018).
[12] M. N. Alexander and D. F. Holcomb, Rev. Mod. Phys. **40**, 815 (1968).
[13] K. A. Chao, F. A. Oliveira, and N. Majlis, Solid State. Commun. **21**, 845 (1977).
[14] B. I. Shklovskii, Phys. Rev B **73**, 193201 (2006).
[15] M. Römer, H. Bernien, G. Müller, D. Schuh, J. Hübner, and M. Oestreich, Phys. Rev. B **81**, 075216 (2010).
[16] J. G. Lonnemann, E. P. Rugeramigabo, M. Oestreich, and J. Hubner, Phys. Rev. B **96**, 045201 (2017).
[17] P. I. Tamborenea, D. Weinman, and R. A. Jalabert, Phys. Rev. B **76**, 085209 (2007).
[18] G. A. Intronati, P. I. Tamborenea, D. Weinmann, and R. A. Jalabert, Phys. Rev. Lett. **108**, 016601 (2012).
[19] T. Matsubara and Y. Toyozawa, Prog. Theor. Phys. **26**, 739 (1961).
[20] T. Wellens and R. A. Jalabert, Phys. Rev. B **94**, 144209 (2016).
[21] W. O. Putikka and R. Joynt, Phys. Rev. B **70**, 113201 (2004).
[22] D. Paget, Phys. Rev. B **24**, 3776 (1981).
[23] N. J. Harmon, W. O. Putikka, and R. Joynt, Phys. Rev. B **79**, 115204 (2009).
[24] N. J. Harmon, W. O. Putikka, and R. Joynt, Phys. Rev. B **81**, 085320 (2010).
[25] M. Chamarro, F. Bernardot, and C. Testelin, J. Phys.: Condens. Matter **19**, 445007 (2007).
[26] J. Tribollet, E. Aubry, G. Karczewski, B. Sermage, F. Bernardot, C. Testelin, and M. Chamarro, Phys. Rev. B **75**, 205304 (2007).

[27] P. Grinberg, F. Bernardot, B. Eble, G. Karczewski, C. Testelin, and M. Chamarro, J. Appl. Phys. **119**, 123906 (2016).
[28] D. J. Sleiter, K. Sanaka, Y. M. Kim, K. Lischka, A. Pawlis, and Y. Yamamoto, Nano Lett. **13**, 116 (2013).
[29] J. Kainz, U. Rössler, and R. Winkler, Phys. Rev. B **70**, 195322 (2004).
[30] B. Siarry, B. Eble, F. Bernardot, P. Grinberg, C. Testelin, M. Chamarro, and A. Lemaître, Phys. Rev. B **92**, 155315 (2015).
[31] K. V. Kavokin, Phys. Rev. B **69**, 075302 (2004).
[32] L. P. Gor'kov and P. L. Krotkov, Phys. Rev. B **67**, 033203 (2003).
[33] N. W. Aschroft and D. Mermin, *Solid State Physics* (Brooks-Cole, Belmont, 1976).
[34] J. Tribollet, F. Bernardot, M. Menant, G. Karczewski, C. Testelin, and M. Chamarro, Phys. Rev. B **68**, 235316 (2003).
[35] A. T. Neal *et al.*, Appl. Phys. Lett. **113**, 062101 (2018).
[36] G. M. Castellan and F. Seitz, *Semiconducting Materials* (Butterworths, London, 1951).
[37] I. V. Osinnykh, K. S. Zhuravlev, T. V. Malin, B. Y. Ber, and D. Y. Kazantsev, Semiconductors **48**, 1134 (2014).
[38] N. F. Mott, *Metal-Insulator Transitions* (Taylor and Francis, London, 1990).
[39] A. Tackeuchi, T. Kuroda, S. Muto, Y. Nishikawa, and O. Wada, Jpn. J. Appl. Phys. **38**, 4680 (1999).
[40] G. Fonthal, L. Tirado-Mejia, J. I. Marin-Hurtado, H. Ariza-Calderon, and J. G. Mendoza-Alvarez, J. Phys. Chem. Solids **61**, 579 (2000).